scientific reports

Check for updates

OPEN

# Increased activation of the WNT pathway in brain tissue from patients with cortical dysplasia type IIb

Fabio Jean Varella[1,2], Fernando Antônio Costa Xavier[1,2], Gabriele Zanirati[1], João Ismael Budelon Gonçalves[1], Thales Thor Ramos Previato[1,4], Douglas Bottega Pazzin[1,2], Normando G. Pereira-Neto[5], Eliseu Paglioli[5], William Alves Martins[5], Andre Palmini[5], Adriana Souza dos Santos[7], José Garcia Abreu[6], Kamila Souto Leichtweis[6], Denise C. Machado[1], Jaderson Costa Da Costa[1] & Daniel Rodrigo Marinowic[1,2,3,4]✉

**Focal cortical dysplasia (FCD) is a malformation of cortical development characterized by a heterogeneous group of lesions with high epileptogenic activity. Somatic mutations in the mTOR pathway are the primary cause of cortical malformations (MCDs). Activation of the WNT pathway inhibits GSK3, which is a key inhibitor of mTOR; consequently, WNT activation is associated with increased activation of the mTOR pathway. Residual samples were obtained from the neocortex of five patients diagnosed with FCD type IIb who underwent surgery. For the control group, residual samples from the neocortex of 3 patients with temporal lobe epilepsy associated with hippocampal sclerosis (TLE-HS) were used. The samples were used to evaluate relative gene expression levels, immunohistochemical characteristics, and the quantification of proteins related to the WNT pathway by Western blot. Gene expression analysis showed increased fold-changes in the genes LRP5, LRP6, DKK1, and DVL1. Immunohistochemistry analysis revealed that the FCD brain samples exhibited more staining for LRP6 compared to control brain tissue. All patients with FCD showed stronger staining for β-catenin. The increased gene expression of WNT pathway genes, combined with the intensified anti-LRP6 antibody staining and increased β-catenin staining, along with the reduced rate of β-catenin phosphorylation observed in patients with FCD, suggests a more pronounced activation of the WNT pathway.**

**Keywords** Focal cortical dysplasia, WNT pathway, Epilepsy, Beta-catenin, LRP5, LRP6

Focal Cortical Dysplasia (FCD) is a malformation of the cerebral cortex accompanied by lesions with high epileptogenic activity and is one of the main causes of refractoriness to drug treatment[1]. Its origin may be related to disturbances in neuronal proliferation and differentiation, resulting in a series of visible structural abnormalities in the cortical layers, which may or may not be accompanied by dimorphic neurons and balloon cells[2,3].

FCD is highly heterogeneous and can affect any region of the cortex. The most recent histological classification of FCD, proposed in 2022 by the International League Against Epilepsy (ILAE), distinguishes between FCD types I and II, which are characterized by cortical delamination and structural abnormalities. FCD type IIA presents with only dysmorphic neurons, whereas FCD type IIb is characterized by the presence of both dysmorphic neurons and balloon cells. FCD type III is associated solely with cortical delamination and specific structural lesions, and is subdivided into four types: hippocampal sclerosis, brain tumors, vascular malformations, and

[1]Brain Institute of Rio Grande do Sul (BraIns), Pontifical Catholic University of Rio Grande do Sul, Porto Alegre, Brazil. [2]Graduate Program in Medicine and Health Sciences, Medical School, Pontifical Catholic University of Rio Grande do Sul, Porto Alegre, Brazil. [3]Graduate Program in Medicine, Pediatrics and Child Health, Medical School, Pontifical Catholic University of Rio Grande do Sul, Porto Alegre, Brazil. [4]Graduate Program in Biomedical Gerontology, Medical School, Pontifical Catholic University of Rio Grande do Sul, Porto Alegre, Brazil. [5]Epilepsy Surgery Program, São Lucas Hospital, Pontifical Catholic University of Rio Grande do Sul, Porto Alegre, Brazil. [6]Biomedical Science Institute, Universidade Federal do Rio de Janeiro, Rio de Janeiro, Brazil. [7]Federal University of Rio Grande do Sul, Porto Alegre, Brazil. ✉email: daniel.marinowic@pucrs.br

lesions acquired early in life[4]. Somatic mutations are the primary cause of cortical malformations (MCDs), particularly FCD, and are found at varying frequencies, predominantly affecting the mTOR pathway (AKT3, DEPDC5, mTOR, TSC1, TSC2)[2]. The Wnt/β-catenin pathway plays a key role in the development of the cerebral cortex by mediating processes of cell migration, cell proliferation, and cell fate specification, as well as maintaining the balance between cell proliferation and differentiation in the ventricular zone[5–7]. The TSC complex is one of the main inhibitors of the mTOR pathway by suppressing RHEB activity. The activated WNT pathway inhibits GSK3 (a protein kinase that suppresses the mTOR pathway) and consequently contributes to mTOR pathway activation[8]. Considering the importance of this pathway, new studies have been conducted to better understand the Wnt/β-catenin pathway in FCD. A study by Marinowic et al. found molecular changes in the Wnt pathway in dysplastic and perilesional tissue that were predictive of seizures in patients[9].

The main mechanism of action of the Wnt/β-catenin pathway is the inactivation of the β-catenin protein destruction complex, leading to the accumulation of β-catenin in the cytoplasm[10]. In the absence of Wnt pathway signal transduction, β-catenin is degraded by a multiprotein complex. The activation signals of the canonical pathway are transmitted through the binding of the Wnt protein to seven-pass transmembrane Frizzled (FZD) receptors and to the low-density lipoprotein receptor-related protein-5 or -6 (LRP5/6 coreceptors). This interaction promotes the recruitment of the Dishevelled protein (DVL), establishing conditions for the inactivation of the β-catenin destruction complex. This mechanism inactivates the GSK3β protein, resulting in the release of β-catenin from the multiprotein destruction complex[11]. As a result, cytoplasmic β-catenin levels increase and translocate to the nucleus, where it interacts with the TCF/LEF complex, allowing the transcription of several genes responsible for regulating the cell cycle, proliferation, and cell adhesion. Dickkopf-related protein 1 (DKK1) is the main inhibitor of the Wnt/β-catenin pathway, and its C-terminal region binds to one of the four helices of LRP5/6, inhibiting the pathway[12,13].Increase in WNT and c-MYC protein levels was observed in balloon cells and giant neurons in patients with FCD types IIa and IIb when compared to controls. This process is believed to be related to abnormal cellular and structural formation in the analyzed patients with FCD[14].

Here, we aimed to identify gene expression changes in the WNT signaling pathway in brain samples from patients with FCD type IIB. We focused primarily on the WNT pathway genes LRP5, LRP6, DKK1, and DVL1. We also assessed LRP5 protein levels on the cell surface and intracellular beta-catenin, including its phosphorylation rate. To correlate gene expression differences with clinical manifestations, we relied on patient records from the pre- and post-surgical phases.

## Methods

### Accordance statement

This study was approved by the Research Ethics Committee of the Pontifical Catholic University of Rio Grande do Sul (CAAE: 19776619.9.0000.5336, approval number: 3.577.035). All participants signed a free and informed consent form. All methods were performed in accordance with relevant guidelines and regulations and in accordance with Resolution No. 466/12 of the National Health Council of Brazil. For patients under 18 years of age, the form was signed by their parents or guardians.

### Description of participants

Patients underwent the standard treatment offered in the epilepsy surgery program. In the control group, the decision to perform an anterior temporal lobectomy instead of an amygdalohippocampectomy was made by the program's medical team without the participation of the researchers. All patients or their guardians authorized the use of their biological material for research. No additional cortical fragments were removed during surgery. All patients involved had refractory epilepsy and were referred to the Epilepsy Surgery Program at Hospital São Lucas da PUCRS for resective surgery due to conditions of FCD (dysplasia group) and TLE-HS (control group). The clinical and demographic data of the patients are described in Table 1.

### Sample collection

Samples from the target population were obtained from different regions of the cerebral cortex of 5 patients (4 male and 1 female) aged 9 to 33 years who underwent surgery in the epilepsy program at Hospital São Lucas da PUCRS and were diagnosed with FCD, with histological evidence of FCD type II. Control group samples were obtained from the neocortex of 3 patients with temporal lobe epilepsy associated with hippocampal sclerosis (TLE-HS) who underwent anterior temporal lobectomy. The samples from the control group were histologically characterized as normal cortical tissue.

### RNA extraction and cDNA synthesis

RNA was extracted using the SV-Total RNA Isolation System kit (Promega, Madison, Wisconsin, USA) according to the manufacturer's instructions. The extracted RNA was then converted into cDNA using the GoScript Reverse Transcriptase kit (Promega) following the manufacturer's instructions. Subsequently, the cDNA was quantified using a NanoDrop spectrophotometer to determine the recommended concentration for qRT-PCR analysis.

### qPCR

qPCR assays were performed using the PowerUp SYBR Green kit (Applied Biosystems) according to the manufacturer's instructions. Each reaction was conducted in duplicate, with an initial concentration of 20 ng of cDNA added to the master mix. Real-time PCR was performed using a StepOne Plus system (Thermo Fisher Scientific, Massachusetts, USA). Primers for the LRP5, LRP6, DKK1, and DVL1 genes were designed using the NCBI Primer-BLAST platform. The assays for each gene were conducted in 96-well plates, with NSE and ACTB genes used as endogenous expression controls. The sequences of the primers used are described in Table 2.

| Participant (origin) | FCD1 | FCD2 | FCD3 | FCD4 | FCD5 | TLE-HS 1 | TLE-HS 2 | TLE-HS 3 |
|---|---|---|---|---|---|---|---|---|
| Age at onset' | 25 years | 8 years | 15 years | 8 years | 1 year | 23 years | 28 years | 16 years |
| Seizure types | Convulsions with staring and nonspecific sounds during sleep. Hypermotor seizures | Seizures during sleep, screaming followed by blinking. There is no loss of consciousness or muscle movements (tonic-clonic). Upper limb hypertonia (upper limbs). | Seizures with sensory aura on the right and evolution with simple motor crisis on the right and tonic-clonic crises | Asymmetric tonic attacks with extension of the right arm and right leg | Generalized tonic-clonic seizures during sleep and daily in times of stress. Tonic seizures of the left hemibody | Disconnection, altered thinking, aggression, and verbal outbursts; at times, wandering aimlessly | Generalized tonic-clonic seizures during sleep | Aura, automatisms, and epigastric discomfort |
| Seizure frequency | 3–4 daily seizure | 3–4 daily seizure | 2–3 daily seizure | 2 daily seizure | Each 3 days | | | |
| EEG | Continuous epileptform paroxysms in the left frontal region | Paroxysms and parietal epileptic seizures on the right | Parietal and occipital paroxysms on the lef | Left frontal paroxysms | Left parietal-center epileptiform activity | Right temporal lobe seizures | Epileptiform discharges in the right temporal lobe | Irritative activity in the right anterior temporal region |
| MRI findings (age at investigation) | Transmantic dysplasia in the upper and middle frontal region | Signal change and blurring of the white matter and cortico-subcortical interface of the right parieto-occipital transition | Change in signal and blurring of the cortico-subcortical interface of the left parietal lobe and transmantic dysplasia, compatible with malformation of cortical development | Thickening and changes in the cortico-subcortical transition of the left middle frontal gyrus with transmantle sign | Cortical thickening in the left parietal lobe with alteration of cortical gyri | Right mesial temporal sclerosis | Atrophy and signal alteration in the right hippocampus | Right mesial temporal sclerosis |
| Surgical resection area | Left frontal region | Right occipital parietal region | Left parietal region | Right frontal region | Letf sensitive girus region | – | – | – |
| Histology | IIB | IIB | IIB | IIB | IIB | No change* | No change* | No change* |
| Postoperative outcome | There are no clinical complications or epileptic seizures after surgery. Engel IA | There are no clinical complications or epileptic seizures after surgery. Engel IA | No seizures after surgery Engel IA | No seizures after surgery Engel IA | Had auras after surgery, currently 20 months without attacks Engel IB | No seizures after surgery | No seizures after surgery | No seizures after surgery |

**Table 1**. Table with clinical data of study participants. *EEG* electroencephalogram, *MRI* magnetic resonance imaging. *No histologic change in cortical sample used.

| Genes | Sequence |
|---|---|
| LRP5 | Forward: GGACACCAACATGATCGAGTCG<br>Reverse: CGCTCAATGCTGTGCAGATTCC |
| LRP6 | Forward: CAGTTGGAGTGGTGCTGAAAGG<br>Reverse: CCATCCAAAGCAGCCCGTTCAA |
| DKK1 | Forward: GGTATTCCAGAAGAACCACCTTG<br>Reverse: CTTGGACCAGAAGTGTCTAGCAC |
| DVL1 | Forward: GACCCTGTCATCTGTCCCAC<br>Reverse: TTCAGACTGTTGCCGGATGG |
| NSE | Forward: CTGTATCGCCACATTGCTCAGC<br>Reverse: AGCTTGTTGCCAGCATGAGAGC |
| ACTB | Forward: CACCATTGGCAATGAGCGGTTC<br>Reverse: AGGTCTTTGCGGATGTCCACGT |

**Table 2**. Primer sequences used in the PCR.

## Immunohistochemistry

The samples were fixed in 4% paraformaldehyde (PFA) in 0.1 M phosphate buffer (pH 7.4) for 24 h at room temperature. They were then dehydrated and infiltrated with paraffin through 12 subsequent baths (4% PFA, 70% alcohol, 80% alcohol, 90% alcohol, 96% alcohol twice, xylene three times, and paraffin three times), each for 1 h. The samples were then embedded in paraffin and stored at room temperature.

## IHC staining

Slides were cut at 5 µm and fixed onto histological slides coated with (3-Aminopropyl) triethoxysilane. Deparaffinization was performed through subsequent baths in xylene (twice), 90% alcohol, 80% alcohol, 70% alcohol, and distilled water, with each bath lasting 5 min. Antigen retrieval was carried out in PBS at 70 °C for 40 min, followed by blocking of nonspecific binding with a buffer containing 1% BSA, 5% SFB, and 0.2% Triton X-100 at room temperature for 30 min. The slides were then washed with PBS and incubated with the primary

antibody (Rabbit Anti-LRP5, 1:200) diluted in buffer solution (1% BSA, 5% SFB, 0.2% Triton X-100) (100 µL per slide) at 4 °C overnight. The slices were washed with PBS and incubated with the secondary antibody (Goat Anti-Rabbit Alexa Fluor™ 633 – A21070, 1:200) diluted in buffer solution (1% BSA, 5% SFB, 0.2% Triton X-100) (100 µL per slide) at room temperature for 1 h. Finally, the slices were exposed to 4',6-Diamidino-2-Phenylindole Dihydrochloride (DAPI) for 5 min, followed by fixation with Canada balsam.

For each evaluation, 20 visual fields were randomly captured using a 200x magnification. The images were quantified using the area (pixel) markup parameter for the LRP5 marker. For the Nuclear Morphometric Analysis, the parameters used were area, aspect ratio, bounding box area, radius ratio, and roundness for the DAPI marker, analyzed with Image-Pro Plus 7.0 software.

### Western blotting

Cortex tissues from patients with FCD were lysed using RIPA buffer (50 mM Tris-HCl, pH 7.5; 150 mM NaCl; 0.5% sodium deoxycholate; 0.1% SDS; 1 mM EDTA; 1% Triton X-100; 10% glycerol) and phosphatase/protease inhibitors (Pierce™ Protease and Phosphatase Inhibitor Mini Tablets, Waltham, MA, USA, #A32959) for 30 min, followed by centrifugation for 15 min at 400 x g at 4 °C. Tissue lysates were then mixed with Laemmli buffer (2% SDS, 10% glycerol, 5% 2-mercaptoethanol, 0.002% bromophenol blue, and 125 mM Tris-HCl, pH 6.8) and heated at 95 °C for 5 min. The protein concentration was quantified using Qubit™ Protein Assay Kits (Thermo Fisher Scientific, Massachusetts, USA), and 40 µg of protein was used for each run. Protein samples were separated on SDS-PAGE gels and transferred to Immobilon-E membranes (Millipore, Burlington, MA, USA, #IEVH85R). The membranes were blocked for 1 h with TBS-T containing 2% PVP (Polyvinylpyrrolidone, Sigma, Burlington, MA, USA), and then incubated with a primary antibody for 1 h at room temperature or overnight at 4 °C. The primary antibodies used for Western blot analysis included anti-β-catenin – 85 kDa (1:500, MA5-15569 - Thermo Fisher Scientific, Massachusetts, USA), anti-phosphorylated β-catenin – 85 kDa (1:500, #702374 - Thermo Fisher Scientific, Massachusetts, USA), and anti-GAPDH – 42 kDa (1:3000, AM4302, Invitrogen). The Precision Plus Protein™ ladder, ranging from 10 kDa to 250 kDa (Bio-Rad, catalog no. 1610373), was used as the molecular weight marker. After three washes with TBS-T, the membranes were incubated for 1 h with HRP-conjugated secondary antibodies (CST). The membranes were visualized by chemiluminescence using SuperSignal West Pico and West Femto (Thermo Fisher, Life Technologies Corporation, Carlsbad, CA, USA). Band intensities were quantified using ImageJ (National Institutes of Health, Bethesda, Maryland, USA) analysis software.

### Data analysis

For analysis of the gene expression profile, ΔΔCt values were calculated using the Ct values of the NSE and ACTB genes as endogenous controls, compared to the Ct values of the target genes (DKK1, LRP5, LRP6, and DVL1). Samples from healthy brain tissue were used as reaction controls, while samples from brain tissue with FCD were assigned to the research group. The $2^{-\Delta\Delta Ct}$ method was used for HR generation. For gene expression analysis, differences between specific points were determined via Student's t-test for normal distribution. Additionally, an evaluation of the $2^{-\Delta Ct}$ values for each analyzed sample was performed, allowing for the construction of a heatmap and a correlation map.

The LRP5 marker area was calculated as the ratio of the area in pixels to the number of labeled cell nuclei in each field. The nuclear morphometric analysis (NMA) was used to assess characteristics related to nuclear morphology and size in order to map the population dynamics of cell nuclei from patients who are LRP5 positive and negative for FCD.

For the Western blotting analysis, band intensity values were used for normalization through the ratio of GAPDH to β-catenin and phosphorylated β-catenin. For the analysis of β-catenin expression, the ratio of total to phosphorylated β-catenin was calculated to demonstrate the activation of the WNT pathway. Additionally, the percentage of β-catenin phosphorylation was calculated for the two groups analyzed. The Shapiro–Wilk and Anderson–Darling tests were used to determine data normality, and the Levene test was employed to assess data variance. The results indicated that the data were parametric and that the variances were not equal. Consequently, Welch ANOVA, followed by the Games-Howell post hoc test, was used.

## Results

### Gene expression

Analysing the fold-change values of the FCD group generated from the $2^{-\Delta\Delta Ct}$ equation using the cortical tissue of participants who underwent hippocampectomy (control tissue), there was an increase in the expression of the genes LRP5, LRP6, DKK1, and DVL1.

The mean $2^{-\Delta\Delta Ct}$ values for the FCD group were 2.25 for the LRP5 gene, 2.27 for LRP6, 2.23 for DKK1, and 1.58 for DVL1 (Fig. 1A). The comparison of the $2^{-\Delta Ct}$ results between the FCD and control tissues was performed using $2^{-\Delta Ct}$ values. The results, presented as a heatmap, showed different of $2^{-\Delta Ct}$ values in the FCD brain tissue compared to the control brain tissue for the LRP5, LRP6, DKK1, and DVL1 genes (Fig. 1B). The $2^{-\Delta Ct}$ showed in the heatmap format were used solely to illustrate the differences between groups (control and DCF) as well as intragroup variations. The histological characterization of controls and FCD patients was confirmed using hematoxylin and eosin staining of cortical tissue samples, which demonstrated the presence of balloon cells (arrows) in the FCD tissue (Fig. 1C and D).

### Immunohistochemistry

Patients with FCD showed stronger anti-LRP5 antibody staining (Fig. 2A, B and C). The area marked in pixels per nucleus was 4.54 pixels, which was significantly different from the area marked in the control tissue, which was 0.41 pixels ($p = 0.0101$). The labeled area represents the ratio between the number of nuclei and the amount

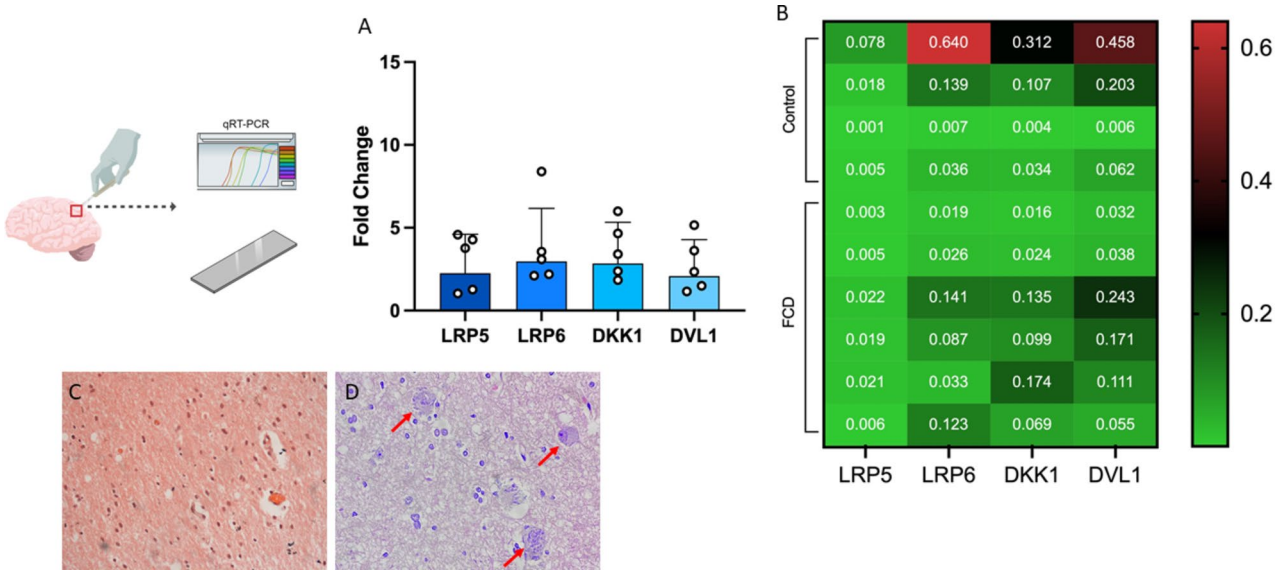


**Fig. 1**. Gene expression analysis of samples from patients with FCD: (**A**) Relative expression analysis using the $2^{-\Delta\Delta Ct}$ calculation showing increased expression of the LRP5, LRP6, DKK1, and DVL1 genes in dysplastic cortical tissue. (**B**) Heatmap constructed using $2^{-\Delta Ct}$ values showing differences in the expression profiles of samples from the FCD group compared to the control group. Histological sections stained with hematoxylin and eosin of cortical tissue samples from a control patient (**C**) and an FCD patient (**D**), showing the characterization and presence of balloon cells (arrows) in the FCD tissue. The Student's t test was used to determine statistical significance. Error bars represent SEM.

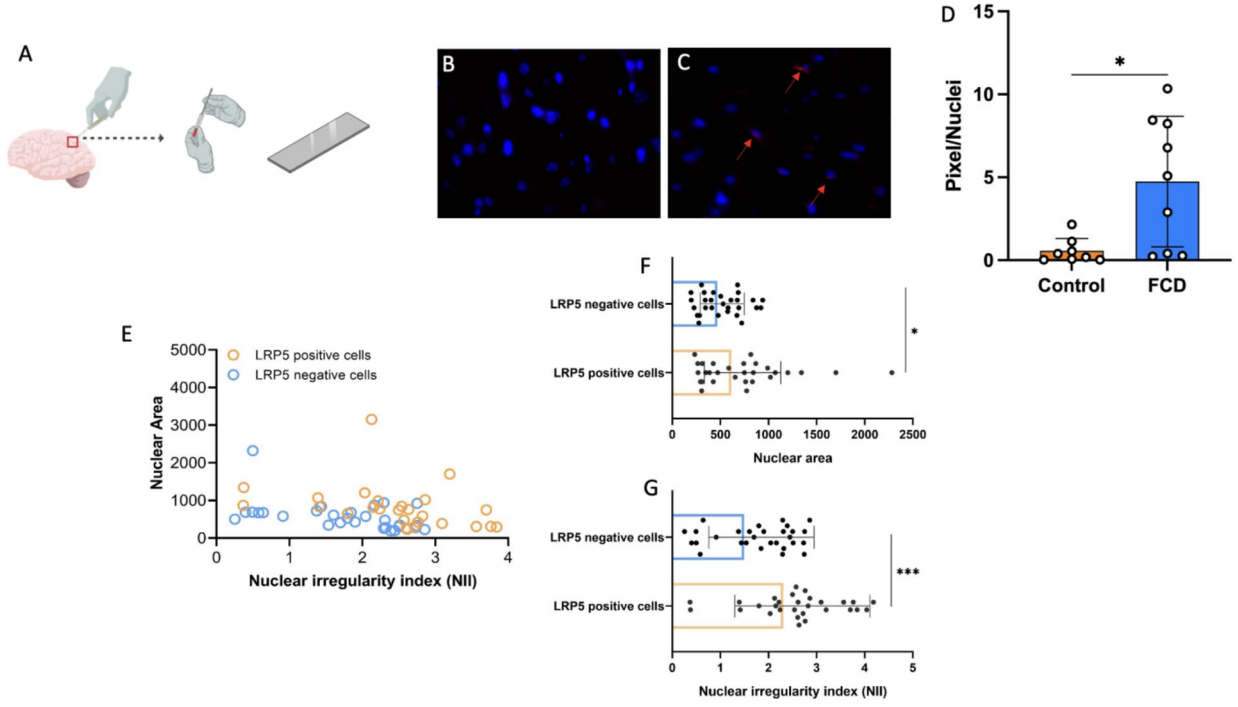


**Fig. 2**. Immunohistochemical analysis of cortical tissue: (**A**) Fluorescence immunohistochemistry protocol showing LRP5 staining in the cortical tissue of control (**B**) and FCD (**C**) samples (in blue: DAPI-labeled nuclei; in red: LRP5 staining). (**D**) Graphical representation of the increase in LRP5 staining in patients with FCD after quantification of marked area of 20 random fields. (**E**) Distribution of nuclei in a plot of area versus NII in FDC tissue. Comparison of the population distribution of LPR5 positive and negative cells by area (**F**) and NII (**G**). The asterisks above the graphs indicate statistical significance as follows: $*0.01 < p < 0.05$, $**0.001 < p < 0.01$, $***p < 0.001$. The t test was used to determine statistical significance. Error bars represent the standard error of the mean (SEM).

of staining in each captured field (Fig. 2D). The nuclear morphometric analysis (NMA) showed differences in nuclear phenotypes (Nuclear Irregularity Index - NII) between the FCD cells with LRP5 positive and LRP5 negative immunohistochemistry marker (Fig. 2E), where the LRP5 positive cell group showed the highest mean concentration of nuclei with larger areas (Fig. 2F). However, it is noticeable that the population concentration of LRP5 negative cells shows a more homogeneous distribution of nuclear area when compared to the LRP5 positive cell group (Fig. 2G). The reference values are described in Table 3.

### Western blotting

Brain tissue samples from patients with FCD showed increased β-catenin staining compared to the control. In the control group, the values for total β-catenin and phosphorylated β-catenin were very similar, with the calculated phosphorylation percentage being 97.5%. In FCD, there was a difference between total and phosphorylated β-catenin, resulting in a phosphorylation percentage of 65.7%. This difference was statistically significant between the groups ($p = 0.008$). The higher concentration of unphosphorylated β-catenin indicated that the canonical WNT pathway was more active in dysplastic brain tissue (Fig. 3). The full western blot gel image is present in Supplementary Figure S1.

## Discussion

The increased activity of the WNT pathway may be crucial for gaining a clearer understanding of the pathophysiology of epileptic seizures in patients with FCD. Although our results indicate increased WNT pathway activity in these subjects, the impact of this pathway's activation in epileptogenesis requires further investigation to be elucidated.

Specifically, in relation to epilepsy, the focus of research on the WNT pathway has been its relationship with the control mechanisms of neurogenesis induced by seizures and neuronal death in both the acute and chronic phases of the disease. Using various methods to induce seizures, several studies have found that elevated expression of WNT pathway components is associated with increased aberrant neurogenesis and neuronal death commonly observed following seizures[15]. Modulation of the interaction between WNT receptors presents great potential as a therapeutic target for many diseases, such as osteoporosis, multiple myeloma, osteosarcoma, and melanoma[12]. Additionally, modulation of the WNT pathway through DKK has shown protective effects against the progression of hippocampal sclerosis in a kainic acid-induced epilepsy model[16].

Relative expression analysis allows for the identification of differences in the amount of messenger RNA transcribed in the cytoplasm of cells. In this study, we analyzed the expression profiles of the genes LRP5, LRP6, DKK1, and DVL1 in the cortical tissue of patients with FCD type IIb compared to residual cortical tissue from patients with TLE-HS. Changes in gene expression may be due to several factors. The regulation of many genes in humans is related to the response to stimuli or stress, which can induce or reprogram gene transcription. Furthermore, the magnitude and duration of such responses are proportional to the time and severity of the disturbance, considering an individual's exposure to different simultaneous stresses[17].

The cortical tissue of patients with FCD showed a greater staining area for the LRP5 co-receptor. The binding of WNT to Frizzled and LRP5/6 receptors transports the DVL protein to the cell membrane, leading to the phosphorylation of the cytoplasmic tails of LRP5/6, which can then bind to the AXIN protein, removing it from the destruction complex. This causes the complex to disassemble and release β-catenin, thereby activating the WNT pathway[18–20].

Furthermore, we showed that cells labeled for LRP5 exhibit an increased area and NII. Generally, an increase in mean nuclear area can indicate certain physiological conditions of the cells, such as increased proliferation and, consequently, higher metabolic and synthetic activity[21,22]. Moreover, it may also indicate extensive DNA damage[23]. It was also observed that the LRP5 negative cell group is shifted more to the left compared to the LRP5 positive cells (Fig. 2G), which suggests that the nuclei exhibit more regular characteristics. The increase in nuclear size combined with irregularities in shape is often a sign of altered cellular behavior, which can occur under conditions of genomic instability and dysplasia[24,25].

| Comparison of nuclear morphometric parameters between FCD cases and controls | | | | | | |
|---|---|---|---|---|---|---|
| | Mean and standard deviation | | | | | |
| | FCD group | | | Control group | | |
| Nuclear morphometric parameters | With-LRP5 labeling | Without-LRP5 labeling | Value of P | With-LRP5 labeling | Without-LRP5 labeling | Value of P |
| Area | 822.4333333± 636.5202 | 576.4666667 ± 396.9665784 | ns | 495.5 ±222.4794373 | 303.2 ± 117.5157673 | 0.0384 |
| Bounding box area | 324159.1333 ± 246550.0035 | 162385.9333 ± 129530.5935 | 0.0389 | 260382.3333 ±367379.4618 | 419814.9 ± 246489.9753 | ns |
| Width | 31.13333333 ± 13.73576588 | 27.13333333 ± 10.32483893 | ns | 25.83333333 ± 10.47695885 | 21.4 ± 4.742245132 | ns |
| Height | 37.8 ±12.81270921 | 28.06666667 ± 8.403338144 | 0.001 | 30.83333333 ± 12.40026881 | 20.5 ± 3.951089864 | 0.0263 |
| Major | 40.8587 ± 14.01895174 | 30.3047 ± 10.46135271 | 0.0016 | 34.72983333 ± 11.75403596 | 22.5209 ± 4.268802602 | 0.0091 |
| Minor | 23.1252 ± 9.23557122 | 22.42636667 ± 6.024928441 | ns | 18.1455 ± 4.931193314 | 16.6213 ± 3.516048099 | ns |
| Aspect ratio | 1.800933333 ± 0.47099725 | 1.324366667 ± 0.218699997 | < 0.0001 | 2.048333333 ± 1.028353376 | 1.3006 ± 0.239094217 | 0.0411 |
| Roundness | 0.571 ± 0.124664792 | 0.766333333 ±0.109303858 | < 0.0001 | 0.574166667 ± 0.214458776 | 0.7635 ± 0.101826923 | 0.0301 |

**Table 3**. Parameters used to calculate the nuclear morphometric analysis (NMA) on cells with and without LRP5 staining.

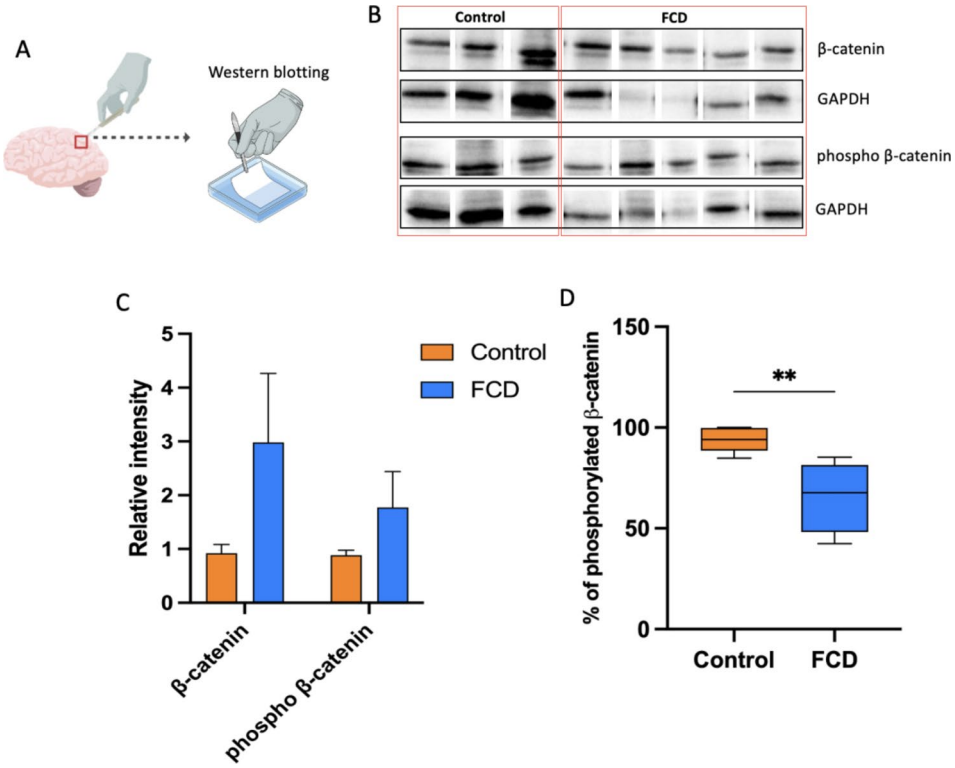


**Fig. 3**. Protein analysis of cortical tissue: (**A**) Western Blotting protocol showing LRP5 staining in the cortical tissue of control and FCD. (**B**) Western blot gel showing corresponding bands for β-catenin and phosphorylated β-catenin. (**C**) Quantification of β-catenin and phosphorylated β-catenin in cortical tissues from control and FCD samples. (**D**) The percentage of phosphorylated β-catenin, determined by the difference between total and phosphorylated β-catenin, showed a lower amount of phosphorylated β-catenin in FCD samples ($p = 0.008$), indicating increased WNT pathway activity. The asterisks above the graphs indicate statistical significance as follows: *$0.01 < p < 0.05$, **$0.001 < p < 0.01$, ***$p < 0.001$. The t test was used to determine statistical significance. Error bars represent the standard error of the mean (SEM).

The severity of drug-resistant epilepsy depends on several variables, such as etiology, seizure type, age at disease onset, time elapsed until surgery, location of the epileptogenic lesion, proximity to eloquent areas, and tolerance and response to medication. The numerous variables involved in the drug-resistant epilepsy phenotype prevent a definitive conclusion regarding the observed differences between the groups. However, we believe that these differences should be considered in future studies and offer a new perspective for evaluating cortical dysplasia[26]. The study by Kalilani et al. evaluated several risk factors related to the development of refractory epilepsy, including age at seizure onset, etiology of epilepsy, and the presence of neuropsychiatric disorders. Additionally, factors such as a history of febrile seizures, status epilepticus, abnormal EEG, and abnormal neuroimaging results were also identified as being associated with an increased risk of refractory epilepsy[27].

Patients with FCD exhibited stronger staining for β-catenin, along with a lower rate of β-catenin phosphorylation, indicating higher activity of the WNT pathway. Regardless of gene expression behavior, the pathway was more active in all analyzed patients with FCD. In an animal model study, adult rats exposed to kainic acid-induced seizures showed increased levels of Wnt3a, β-catenin, and cyclin D1 in the hippocampus, with peak expression of these proteins occurring 14 days after the condition. Another study using a Wnt signaling reporter mouse strain (Topgal mice) revealed that Wnt/β-catenin signaling was increased in reactive astrocytes after focal cortical ischemia[28]. Theilhaber et al. investigated the activation of functional pathways during hypoxic seizures using microarray profiling. The study revealed an increase in the gene expression of several components of the Wnt/β-catenin pathway, including genes for β-catenin (CTNNB1), the inhibitory protein SFRP2, the transducer Dvl3, the co-receptor LRP5/6, and components of the β-catenin regulatory complex such as CSNK1E, GSK3β, Axin2, and APC. Additionally, increases were observed in the gene expression of the ligands Frizzled, Wnt2, Wnt5a, and Wnt10a[29].

Cortical malformation tissue can present as a mosaic with potential distinct genomic alterations, which may result in different changes and phenotypes within the same pathology, especially when alterations occur in a small population of cells or tissue[30]. Heterozygous germline mutations in TSC1 and TSC2 cause Tuberous Sclerosis, while germline mutations in GATOR1 (another mTOR inhibitor) are associated with familial focal epilepsies[31]. The GSK3 protein kinase inhibits the mTOR pathway by phosphorylating TSC2. The activated WNT pathway inhibits GSK3, consequently activating the mTOR pathway. Thus, WNT stimulates translation and cell growth by activating the TSC-mTOR pathway. Moreover, the sequential phosphorylation of TSC2 by

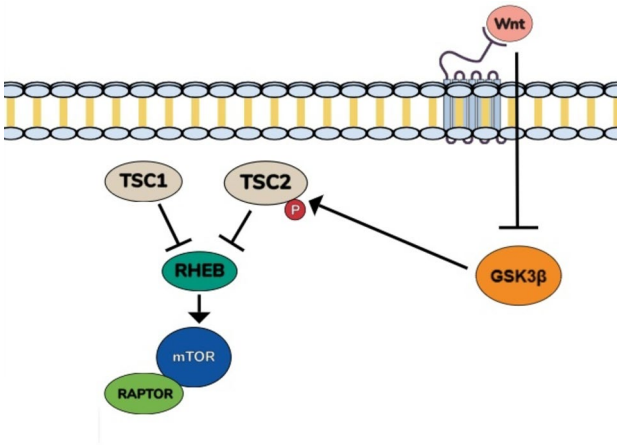


**Fig. 4**. Representation of the WNT pathway influence on mTOR signaling: Increased WNT activity leads to GSK3 inactivation, indirectly enhancing mTOR activation. This occurs because GSK3 inactivation prevents the activation of TSC2, a negative regulator of the mTOR activator Rheb.

AMPK and GSK3 reveals a molecular mechanism for signal integration in cell growth regulation between the WNT and mTOR pathways[8].

Using an alternative pathway such as WNT as a target for understanding and treating refractory epilepsy caused by cortical malformations could be an important tool for achieving success in controlling seizures associated with hyperactivation of the mTOR pathway, for example (Fig. 4).

The development of new antiseizure therapies that are not based on classical mechanisms of action, such as modulating the excitatory-inhibitory balance, has received extensive attention in recent years. Many indirect mechanisms can increase susceptibility to seizures by enhancing connectivity and communication between cells and nervous tissues[26]. Therapeutic alternatives based on signaling pathways are innovative and offer new approaches for controlling seizures and chronic epilepsy[32].

FCDs remain challenging entities, with a low response rate to medical treatments and the need for tailored resections to ensure the removal of all dysplastic lesions while avoiding eloquent regions. The classification of FCDs currently proposed by the ILAE is restricted to histopathological alterations[4]. In the present study, we report significant alterations related to the activation of the WNT pathway in cortical tissue from patients with FCD. However, some limitations must be considered, such as the small number of participants and the use of control samples derived from brain tissue of patients with TLE. An alternative to this control could be the use of normal-appearing adjacent cortex (NACC) tissue (perilesional tissue) from the same patient. However, such resections are performed in very few cases and may share certain transcriptional similarities with dysplastic tissue[9].

The presented results outline an altered molecular profile in FCD patients compared to the control group. However, due to the sample size and the number of variables involved in the disease phenotype, it was not possible to perform an analytical statistical analysis to establish a molecular profile for each patient. The findings of this work, although preliminary, may offer new perspectives regarding diagnosis, classification, and treatment. In neuro-oncology, genetic and molecular criteria, as well as the new classifications of brain tumors, have become the determinants for tumor classification, as biological behavior is more closely related to these variables than to histopathology[33]. In the case of FCDs, the current classification is entirely based on histopathology. This study, although seminal, appears to suggest a similar direction of clinical-biological-molecular correlation, revealing differences in gene expression levels, receptor numbers, and canonical WNT activation in dysplastic brain tissue.

## Data availability

All data generated or analysed during this study are included in this published article [and its supplementary information files].

Received: 3 October 2024; Accepted: 10 February 2025
Published online: 07 March 2025

## References

1. Palmini, A. et al. Intrinsic epileptogenicity of human dysplastic cortex as suggested by corticography and surgical results. *Ann. Neurol.* **37** (4), 476–487 (1995).
2. Brown, W. H., Neill, J. R. O. & Pate, R. R. https://doi.org/10.1007/s00401-019-02061-5 (607), 1–14 (2018).
3. Guerreiro, M. M. Malformations of cortical development. *Arq. Neuropsiquiatr.* **67** (2 B), 570–574 (2009).
4. Najm, I. et al. The ILAE consensus classification of focal cortical dysplasia: an update proposed by an ad hoc task force of the ILAE diagnostic methods commission. *Epilepsia* **63** (8), 1899–1919 (2022).
5. Kilander, M. B. C., Dahlström, J. & Schulte, G. Assessment of Frizzled 6 membrane mobility by FRAP supports G protein coupling and reveals WNT-Frizzled selectivity. *Cell. Signal.* **26** (9), 1943–1949 (2014).
6. Harrison-Uy, S. J. & Pleasure, S. J. Wnt signaling and forebrain development. *Cold Spring Harb. Perspect. Biol.* **4** (7), 1–11 (2012).

7. Noelanders, R. & Vleminckx, K. How wnt signaling builds the brain: bridging development and disease. *Neuroscientist* **23** (3), 314–329 (2017).
8. Inoki, K. et al. TSC2 integrates wnt and energy signals via a coordinated phosphorylation by AMPK and GSK3 to regulate cell growth. *Cell* **126** (5), 955–968 (2006).
9. Marinowic, D.R. et al. WNT pathway in focal cortical dysplasia compared to perilesional nonlesional tissue in refractory epilepsies. *BMC Neurol.* **23** (1), 1–11 (2023).
10. Miller, J. R. Protein family review the wnts. *Gene* 1–15 (2001).
11. Kerekes, K., Bányai, L., Trexler, M. & Patthy, L. Structure, function and disease relevance of wnt inhibitory factor 1, a secreted protein controlling the wnt and hedgehog pathways. *Growth Factors.* **37** (1–2), 29–52 (2019).
12. Cheng, Z. et al. Crystal structures of the extracellular domain of LRP6 and its complex with DKK1. *Nat. Struct. Mol. Biol. [Internet]* **18**(11), 1204–10. https://doi.org/10.1038/nsmb.2139 (2011).
13. Rothbächer, U. & Lemaire, P. Crème De La Kremen of wnt signalling inhibition. *Nat. Cell. Biol.* **4** (7), 172–173 (2002).
14. Kumari, K. et al. mTOR pathway activation in focal cortical dysplasia. *Ann. Diagn. Pathol.* **46**, 151523. https://doi.org/10.1016/j.anndiagpath.2020.151523 (2020).
15. Yang, J. et al. Wnt/β-catenin signaling mediates the seizure-facilitating effect of postischemic reactive astrocytes after pentylenetetrazole-kindling. *Glia* **64** (6), 1083–1091 (2016).
16. Busceti, C. L. et al. Induction of the wnt inhibitor, Dickkopf-1, is associated with neurodegeneration related to temporal lobe epilepsy. *Epilepsia* **48** (4), 694–705 (2007).
17. López-Maury, L., Marguerat, S. & Bähler, J. Tuning gene expression to changing environments: from rapid responses to evolutionary adaptation. *Nat. Rev. Genet.* **9** (8), 583–593 (2008).
18. MacDonald, B. T., Tamai, K. & He, X. Wnt/β-catenin signaling: components, mechanisms, and diseases. *Dev. Cell* **17**(1), 9–26. https://doi.org/10.1016/j.devcel.2009.06.016 (2009).
19. Silva-García, O., Valdez-Alarcón, J. J. & Baizabal-Aguirre, V. M. Wnt/β-catenin signaling as a molecular target by pathogenic bacteria. *Front. Immunol.* **10** (SEP), 1–14 (2019).
20. Qin, K. et al. Canonical and noncanonical Wnt signaling: Multilayered mediators, signaling mechanisms and major signaling crosstalk. *Genes Dis.* **11**(1), 103–34. https://doi.org/10.1016/j.gendis.2023.01.030 (2024).
21. Meng, L. Chromatin-modifying enzymes as modulators of nuclear size during lineage differentiation. *Cell. Death Discov.* **9** (1), 1–11 (2023).
22. Jevtić, P., Edens, L. J., Vuković, L. D. & Levy, D. L. Sizing and shaping the nucleus: mechanisms and significance. *Curr. Opin. Cell. Biol.* **28** (1), 16–27 (2014).
23. Mocali, A., Giovannelli, L., Dolara, P. & Paoletti, F. The comet assay approach to senescent human diploid fibroblasts identifies different phenotypes and clarifies relationships among nuclear size, DNA content, and DNA damage. *J. Gerontol. Ser. Biol. Sci. Med. Sci.* **60** (6), 695–701 (2005).
24. Tejwani, V. et al. PROTAC-mediated conditional degradation of the WRN helicase as a potential strategy for selective killing of cancer cells with microsatellite instability. *Sci. Rep.* **14**(1), 1–16. https://doi.org/10.1038/s41598-024-71160-5 (2024).
25. Terry, N. G. et al. Detection of dysplasia in barrett's esophagus with in vivo depth-resolved nuclear morphology measurements. *Gastroenterology* **140**(1), 42–50. https://doi.org/10.1053/j.gastro.2010.09.008 (2011).
26. Lucke-Wold, B. P. et al. Traumatic brain injury and epilepsy: Underlying mechanisms leading to seizure. *Seizure* **33**, 13–23. https://doi.org/10.1016/j.seizure.2015.10.002 (2015).
27. Kalilani, L., Sun, X., Pelgrims, B., Noack-Rink, M. & Villanueva, V. The epidemiology of drug-resistant epilepsy: a systematic review and meta-analysis. *Epilepsia* **59** (12), 2179–2193 (2018).
28. Qu, Z. et al. Wnt/β-catenin signalling pathway mediated aberrant hippocampal neurogenesis in kainic acid-induced epilepsy. *Cell. Biochem. Funct.* **35** (7), 472–476 (2017).
29. Theilhaber, J. et al. Gene expression profiling of a hypoxic seizure model of epilepsy suggests a role for mTOR and wnt signaling in epileptogenesis. *PLoS One* **8**(9) (2013).
30. McConnell, M. J. et al. Intersection of diverse neuronal genomes and neuropsychiatric disease: The Brain Somatic Mosaicism Network. *Science* **356**(6336) (2017).
31. Baldassari, S. et al. The landscape of epilepsy-related GATOR1 variants. *Genet. Sci.* **21** (2), 398–408 (2019).
32. Huang, C., Fu, X. H., Zhou, D. & Li, J. M. The role of Wnt/β-catenin signaling pathway in disrupted hippocampal neurogenesis of temporal lobe epilepsy: a potential therapeutic target? *Neurochem. Res.* **40** (7), 1319–1332 (2015).
33. Louis, D. N. et al. The 2021 WHO classification of tumors of the central nervous system: a summary. *Neuro Oncol.* **23** (8), 1231–1251 (2021).


## Author contributions

Conceptualization: F.J.V., F.A.C.X., D.R.M., E.P.; Methodology: F.J.V., F.A.C.X., D.R.M., E.P., G.Z., D.C.M.; Writing – original draft: F.J.V., F.A.C.X., D.B.P., D.R.M.; Writing – review & editing: F.J.V., F.A.C.X., G.Z., J.I.B.G., T.T.R.P., D.B.P., N.G.P.N., E.P., W.A.M., A.P., A.S.S., J.G.A., K.S.L., D.C.M., J.C.C., D.R.M.; Data curation: G.Z., W.A.M., A.S.S.; Formal analysis: J.I.B.G., W.A.M.; Investigation: J.I.B.G., J.G.A.; Supervision: D.R.M; E.P.


## Funding

This study was financed in part by the Coordenação de Aperfeiçoamento de Pessoal de Nível Superior (CAPES) – Brazil – Finance Code 001.


## Declarations

## Competing interests

The authors declare no competing interests.

## Additional information

**Supplementary Information** The online version contains supplementary material available at https://doi.org/10.1038/s41598-025-90045-9.

**Correspondence** and requests for materials should be addressed to D.R.M.

**Reprints and permissions information** is available at www.nature.com/reprints.

**Publisher's note** Springer Nature remains neutral with regard to jurisdictional claims in published maps and institutional affiliations.